

Materials Science inc. Nanomaterials & Polymers

Potential Use of DMSA-Containing Iron Oxide Nanoparticles as Magnetic Vehicles against the COVID-19 Disease

Elisama S. Martins,^[a] Ariane Espindola,^[a, b] Tatiane N. Britos,^[a] Camila Chagas,^[c] Emerson Barbosa,^[c] Carlos E. Castro,^[d] Fernando L. A. Fonseca,^[a, c] and Paula S. Haddad^{*(a)}

Iron oxide magnetic nanoparticles have been employed as potential vehicles for a large number of biomedical applications, such as drug delivery. This article describes the synthesis, characterization and in vitro cytotoxic in COVID-19 cells evaluation of DMSA superparamagnetic iron oxide magnetic nanoparticles. Magnetite (Fe₃O₄) nanoparticles were synthesized by co-precipitation of iron salts and coated with meso-2,3-dimercaptosuccinic acid (DMSA) molecule. Structural and morphological characterizations were performed by X-ray

diffraction (XRD), Fourier transformed infrared (FT-IR), magnetic measurements (SQUID), transmission electron microscopy (TEM), and dynamic light scattering (DLS). Our results demonstrate that the nanoparticles have a mean diameter of 12 nm in the solid-state and are superparamagnetic at room temperature. There is no toxicity of SPIONS-DMSA under the cells of patients with COVID-19. Taken together the results show that DMSA-Fe₃O₄ are good candidates as nanocarriers in the alternative treatment of studied cells.

Introduction

COVID-19 is a disease caused by a new strain of coronavirus. Previously, this disease was referred to as "2019 novel coronavirus" or "2019-nCoV". The incubation period of virus infection ranges from 1 to 14 days, being more evident from 3 to 7 days. Fever, dry cough, and fatigue are the main clinical manifestations.^[1] However, the most affected organs are the lungs. With this in mind, developing a vehicle that can carry a drug directly to the lungs is quite interesting hence, a more effective treatment is possible. In this context, new drug delivery nanomaterials that improve the treatment of the COVID-19 consequences are of crucial importance to establish systematic investigation.

Many nanopharmaceuticals has entered clinical practice and even more, are being investigated in clinical trials for a

wide variety of indications.^[2,3] The use for the treatment of viral infections has been observed with promising results.^[4,5] Therefore, the aim of this work was the investigation of nanoparticles for the treatment of COVID-19.

In the last decades, the use of superparamagnetic iron oxide nanoparticles (SPIONs) in biomedicine and pharmaceutical sciences were carefully investigated, especially magnetite nanoparticles (Fe₃O₄), once they have been successfully used in different biomedical applications such as drug delivery, contrast agents for imaging, controlled drug release, hyperthermia, among others.^[6–9] SPIONs present superparamagnetic behavior and act as a single magnetic domain^[10] providing fast response under an external magnetic field and consequently can be guided to a specific target.^[8] In addition, when the magnetic field is removed, no residual magnetization remains, avoiding agglomeration of the nanoparticles in vivo.^[11] This feature permits the guided administration of these nanoparticles to the target tissue/organ with minimum side effects.^[8,12] Bare Fe₃O₄ nanoparticles tend to agglomerate due to magnetic dipole-dipole attractive forces.^[13] Besides that, a high iron concentration in the body affects cell viability, oxidative stress, and other harmfulness.^[14] Therefore, surface functionalization of these nanoparticles with biocompatible molecules is a helpful methodology to avoid nanoparticle agglomeration and permit the conjugation of therapeutic molecules to nanoparticles.^[15–19]


A wide range of works in the literature show that fatty acids such as oleic acid is used to prevent this agglomeration and increase the stability of nanoparticles. Besides that, oleic acid is usually used in iron nanoparticles synthesis due to a protective monolayer formation which induces uniform systems as products.^[20] However, the functionalization with oleic acid generates particles that are dispersed mainly in organic solvents which are generally toxic. Therefore, to propose safe

[a] E. S. Martins, A. Espindola, T. N. Britos, Prof. Dr. F. L. A. Fonseca, Prof. Dr. P. S. Haddad
Department of Chemistry,
Federal University of São Paulo,
Rua São Nicolau, 210. Centro, Diadema, SP, 09961-400, Brazil
E-mail: haddad.paula@unifesp.br

[b] A. Espindola
Institut de Science des Matériaux de Mulhouse (IS2 M),
Université de Haute-Alsace
15 Rue Jean Starcky, 68057 Mulhouse, France.

[c] C. Chagas, E. Barbosa, Prof. Dr. F. L. A. Fonseca
Faculty of Medicine of ABC (FMABC).
Avenida Príncipe de Gales, 667,
Príncipe de Gales, Santo André, SP, 09060-590, Brazil

[d] Dr. C. E. Castro
Center for Natural and Human Science,
Federal University of ABC (UFABC).
Av. dos Estados, 5001 – Bangu, Santo André, SP, 09210-580, Brazil

 Supporting information for this article is available on the WWW under <https://doi.org/10.1002/slct.202101900>

biomedical applications of iron-based magnetic nanoparticles, it must study the biocompatibility of these nanoparticles.^[12,21] Changing the surface of these nanoparticles with biologically active compounds allows the transport of therapeutic agents into specific target cells, increasing specificity and preventing the access of cytotoxic agents to non-target tissues during the delivery process.^[22] Among the biocompatible molecules, meso-2,3-dimercaptosuccinic acid (DMSA) (Figure 1)^[23] is a molecule widely used in the surface coating of magnetite nanoparticles^[24] increasing biocompatibility.^[25]

Studies show that DMSA-coated iron oxide nanoparticles can greatly enhance the rate of cellular acceptance, leading to nonspecific adsorption to the cell surface, followed by endocytosis.^[8,26,27]

Taking advantage of DMSA-SPIONs, in this study, we obtained Fe₃O₄ nanoparticles by the co-precipitation method using ferrous and ferric chlorides in an aqueous solution. Fe₃O₄ magnetic nanoparticles were coated with DMSA (in different mass ratio Fe₃O₄:DMSA) leading to thiolated nanoparticles as potential carried vehicles to COVID 19 treatment to lungs. The physical-chemical and magnetic properties of the nanomaterials were characterized by different techniques. To investigate a possible biomedical application for DMSA-SPIONs, the cytotoxicity in healthy cells and the action on cells of patients with a positive result for Anti-SARS-CoV-2 IgA were analyzed.

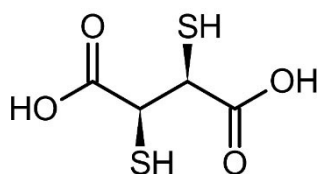


Figure 1. meso-2,3-dimercaptosuccinic acid (DMSA) molecule.^[12]

Results and Discussion

Among several procedures to obtain superparamagnetic iron oxide nanoparticles,^[28–30] the co-precipitation method is one of the most used^[31–33] since it allows acceptable size distribution of water-dispersed SPIONs at room temperature and it is a low-cost method.^[28] It is based on the precipitation of iron salts upon the addition of a weak base in an aqueous solution.^[34] The most common are chemical methods and among those, co-precipitation is widely used to obtain large amounts of hydrophilic nanoparticles. However, SPIONs containing hydrophilic ligand (DMSA) produced directly by this method have a broad size distribution and tend to easily aggregate and become colloiddally unstable. Capping agents such as oleic acid are often used because they form a protective monolayer, which is strongly bonded. This is necessary for making monodisperse and highly uniform nanoparticles. Therefore, nanoparticles with less aggregations are obtained in the presence of oleic acid.^[35,36,37,38,39] The transfer of NPs from the organic to the aqueous phase provides biostability to the particles at physiological pH. Synthetic NPs are generally surface modified with hydrophobic ligands, becoming unstable in aqueous suspension. In this work, the nanoparticles were initially coated with oleic acid and were therefore insoluble in water.

The transfer of nanoparticles from the organic to the aqueous phase offers biostability to the particles at physiological pH.

Figure 2 shows the scheme for the formation of thiolated Fe₃O₄ nanoparticles coated with meso-2,3-dimercaptosuccinic acid (DMSA). It had been used an excess of thiolated ligand in different mass ratios Fe₃O₄:DMSA to total coverage of the Fe₃O₄ surface.

Replacement of oleic acid by DMSA led to SPIONs containing thiol groups on the surface. The amounts of free thiol (–SH) groups on the surface of DMSA-SPIONs (1:5; 1:10 and 1:30) were determined by the reaction of the thiolated

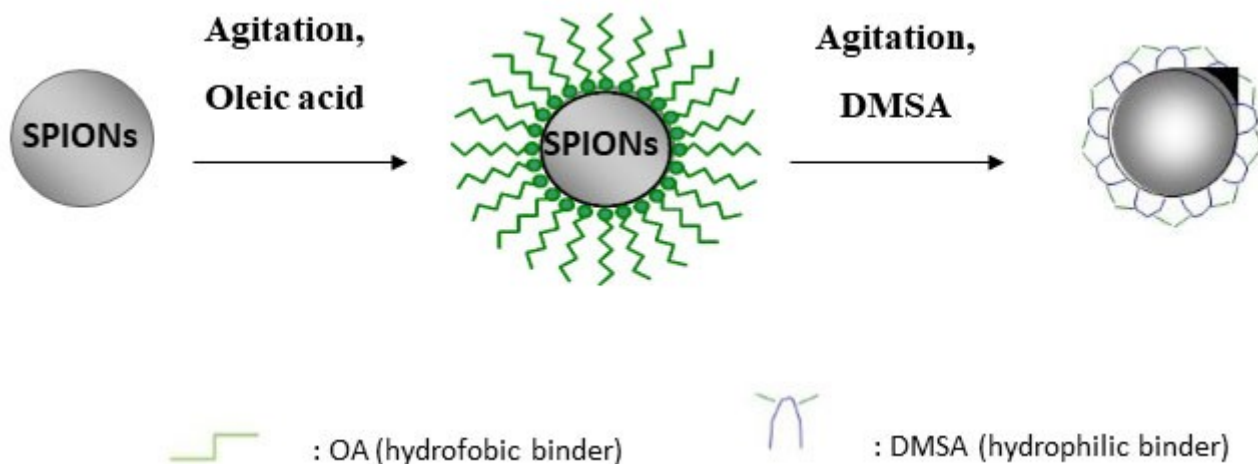


Figure 2. Schematic of the formation of thiolated Fe₃O₄ nanoparticles coated with DMSA.

nanoparticles with a thiol-specific reagent, DTNB.^[16] Values around 0.060 ± 0.008 mmol SH.g⁻¹ of DMSA-SPIONs were found, confirming the presence of free SH groups.

FTIR spectra (Figure 3) show the most important stretching vibrations for the Fe₃O₄ and for the molecules attached to the particle surface. Figure 3A shows the spectra for Fe₃O₄ and OA-Fe₃O₄ nanoparticles. Band assigned to the iron oxide core can be observed at 590 cm⁻¹ (νFe–O). The presence of broadband at 3415.7 cm⁻¹ (νO–H) is attributed to hydroxyl groups on the surface of the nanoparticle. The H–O–H bending and low-intensity band at 1622 cm⁻¹ are indicative of the existence of adsorbed water in surface nanoparticles. On the other hand, for nanoparticles containing oleic acid, the stretching at 1701 cm⁻¹ (νOH), 1611 cm⁻¹ (ν_{asym}COO), and 1424 cm⁻¹ (ν_{sym}COO) are assigned to the carboxylic group.

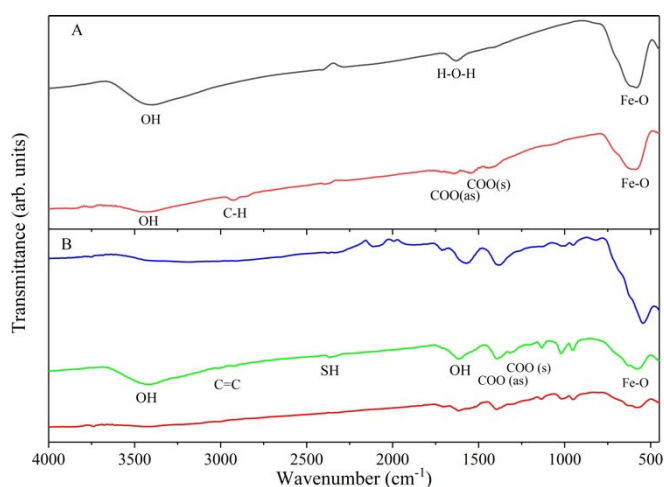


Figure 3. A) FT-IR spectra of Fe₃O₄ nanoparticles (black line) and OA-SPIONs (orange line); B) DMSA-Fe₃O₄ (1:30) (blue line); DMSA-Fe₃O₄ (1:10) (green line); DMSA-Fe₃O₄ (1:5) (red line). in the range of 400–4000 cm⁻¹. The spectra are vertically displaced for better visualization.

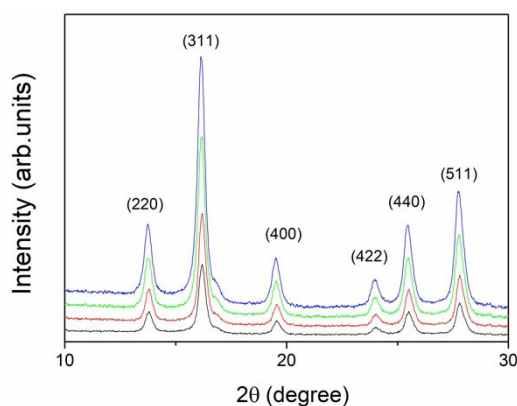


Figure 4. X-ray powder diffraction patterns of OA-Fe₃O₄ nanoparticles (black line), DMSA-Fe₃O₄ nanoparticles (1:5) (red line), DMSA-Fe₃O₄ nanoparticles (1:10) (green line) and DMSA-Fe₃O₄ nanoparticles (1:30) (blue line). The diffractograms were normalized by the maximum peak intensity and vertically displaced for better visualization.

In addition, Figure 3B shows the spectra for the DMSA-Fe₃O₄ nanoparticles and it is possible to note that besides carboxylate groups, two small bands at 2920 and 2980 cm⁻¹ that are attributed to C–H stretching (νC–H) of the DMSA ligand, a band at 931 cm⁻¹ attributed to –CH out of plane bending vibrations of DMSA (δC–H) were observed.^[40,41] The main band of free S–H bond should be observed around 2550 cm⁻¹,^[42] however, it is also possible to observe a dimerization of thiol groups for sample DMSA-Fe₃O₄ (1:10). This fact is in agreement with low values around 0.060 ± 0.008 mmol SH.g⁻¹ of DMSA-Fe₃O₄ nanoparticles.

The X-ray diffractograms for functionalized nanoparticles are shown in Figure 4. The Figure shows the X-ray diffractograms from Fe₃O₄ coated with oleic acid followed by DMSA exchange at molar ratio 1:5; 1:10 and 1:30, respectively, along with their characterization as the inverted spinel structure.^[43] The diffraction peaks refer to a face-centered cubic crystalline structure of the magnetite (Fe₃O₄) (JCPDS#: 110614).^[44] Crystallite sizes from 12 nm were obtained from Scherrer's equation^[30,44] by taking into account the (311) Bragg's reflection.

The morphology of the DMSA-SPIONs (1:5) was analyzed by transmission electron microscopy (Figure 5). It can be observed that the nanoparticles exhibit spherical continuous, however, they present aggregation. The analysis of the TEM image displayed in Figure 5 reveals a broad size distribution with an average size diameter of 14 nm, in agreement with the DRX technique.

Hysteresis isothermal magnetic data (Figure 6) confirmed the superparamagnetic behavior of all nanoparticles. It is observed that the residual magnetization and coercive force were found to be zero for all samples.

The saturation magnetization (M_s) values observed were around 80 emu.g⁻¹ for OA-Fe₃O₄ nanoparticles and 60 emu.g⁻¹ for DMSA-Fe₃O₄. It was possible to note a lower magnetization value for the Fe₃O₄: DMSA (1:5) nanoparticles corroborant the

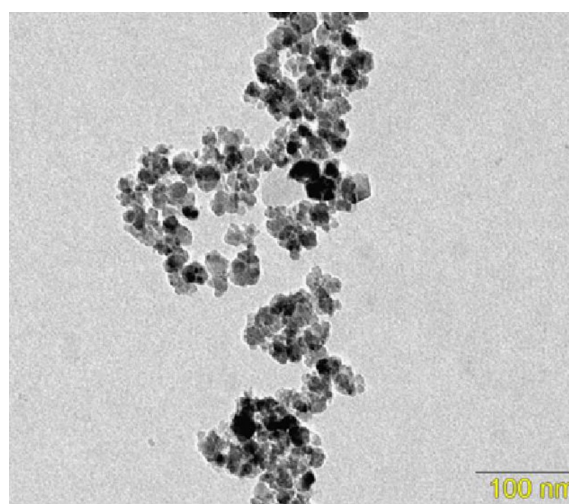


Figure 5. TEM image of DMSA-Fe₃O₄ nanoparticles.

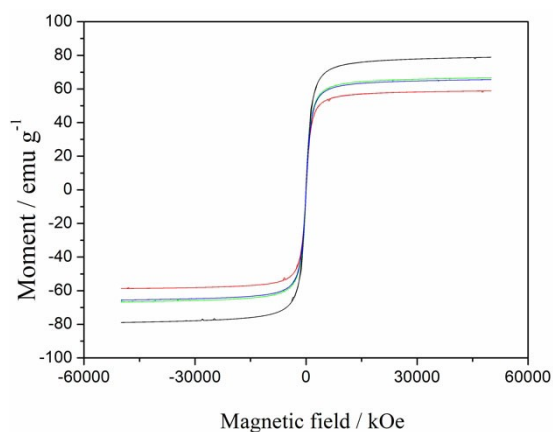


Figure 6. Hysteresis isothermal magnetic of OA-Fe₃O₄ nanoparticles (black line), DMSA-Fe₃O₄ nanoparticles (1:5) (red line), DMSA-Fe₃O₄ nanoparticles (1:10) (green line) and DMSA-Fe₃O₄ nanoparticles (1:30) (blue line).

smaller functionalization of DMSA onto SPIONs surface leaves the core more exposed decreasing the magnetization value.

The synthesis of DMSA-Fe₃O₄ produced a system with a low degree of aggregation when in dispersion, thus resulting in high stability. The quantitative data related to the scattering characterization is displayed in Table 1.

As well-established, higher hydrodynamic sizes of nanoparticles measured by DLS, in comparison with the sizes obtained by XRD and TEM, are attributed to the presence of extra hydrate layers in aqueous environments.^[45] It is worth noting that a PDI value less than 0.2 indicates a homogenous and monodisperse population of nanoparticles.^[46] The zeta potential of DMSA-Fe₃O₄ nanoparticles (-35.0 ± 0.3) mV indicates high colloidal stability.^[47]

Regarding biological assay, several promising studies deal with the use of nanoparticles in diseases caused by viral infections.^[2] There are studies with iron nanoparticles against the influenza virus (H1 N1),^[48] Rotavirus,^[49] and even against the Dengue virus.^[50] Abo-Zeid in 2020,^[3] based on his findings, formulated the hypothesis that SPIONs would have an antiviral activity through interaction with surface proteins thus interfering with the virus binding or entering the host cell, resulting in the neutralization of it. In addition, a study of anchoring iron oxide nanoparticles in SARS-CoV-2 protein S [50] revealed that there was an efficient interaction between the nanoparticles, forming a stable complex, mainly with the S protein of COVID-19, causing efficient conformational interactions of viral proteins, inhibiting the entry of the virus into host cells and, as consequence, limiting replication.^[3]

Table 1. Data obtained by dynamic light scattering and zeta potential techniques.			
Sample	Hydrodynamic size (nm)	Polydispersity index	Zeta potential (mV)
DMSA-Fe ₃ O ₄	51.0 ± 1.1	0.27 ± 0.02	-35.0 ± 1.5

Figure 7 shows the percent mortality of mononuclear fraction cells (MCF-control) and COVID-19 mononuclear fraction cells (MCF-COVID-19) containing DMSA-Fe₃O₄ nanoparticles.

We can observe that in the cell viability assay it was not possible to detect a significant difference between the control groups (negative cells) and the contaminated cells containing nanoparticles in different concentrations. These results show that in the investigation concentration range there was not of interaction between SPIONs and viral proteins. In addition, there is also an increase in mortality rate with the rise of the iron oxide nanoparticles concentrations, as observed in other studies carried out by our group.^[12]

Therefore, our results demonstrate that there is no toxicity of DMSA-Fe₃O₄ nanoparticles under the cells of patients with COVID-19. Being safe in its application in future studies with anchoring proteins and/or molecules known in the application in patients with SARS-CoV-2 in a way effective, in the delivery of some antiviral substance or in the very act of preventing the virus from binding to the receptor. Thus, with these results of non-toxicity, the DMSA-Fe₃O₄ vehicle is a promising option for further studies as a drug or protein carrier in new COVID-19 therapies.^[2]

Conclusion

This work described the preparation, characterization, and biological assay of DMSA-Fe₃O₄ as a potential drug-delivery platform for COVID 19 treatment. Nanoparticles were prepared through the co-precipitation method and coated with DMSA molecule leading to the formation of a stable aqueous dispersion of thiolated nanoparticles. Free thiol groups of DMSA can be used as sites to covalently bind antibiotics or other drugs to the treatment of COVID 19 disease. This drug-releasing nanomaterial might find important biomedical applications. The biological assay carried out had the goal of verifying the cell viability of two different clinical situations. What has been reported is that there is no difference in cell mortality when different concentrations are applied in the evaluated cases.

Taken together the results of non-toxicity showed that DMSA-Fe₃O₄ nanoparticles are a promising option for further studies, with tests for a drug or protein carrier for new therapies for COVID-19.

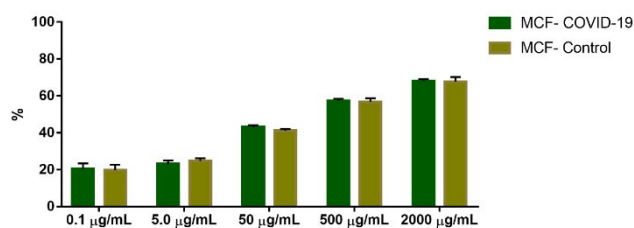


Figure 7. Analysis of mononuclear fraction mortality.

Supporting Information Summary

The supporting information file contains all the experimental procedures describing the synthesis, physicochemical characterizations and biological assays.

Acknowledgments

This work was supported by the São Paulo Research Foundation–FAPESP [grant numbers 2017/15061-6, 2018/12219-0 and 2019/07454-3]. The authors also thank the Multiuser Experimental Center (CEM) of the Federal University of ABC for use of its facilities.

Conflict of Interest

The authors declare no conflict of interest.

Keywords: biocompatibility · COVID-19 · drug delivery · iron oxide · nanoparticles

- [1] K. L. Shen, Y. H. Yang, R. M. Jiang, T. Y. Wang, D. C. Zhao, Y. Jiang, X. X. Lu, R. M. Jin, Y. J. Zheng, B. P. Xu, Z. De Xie, Z. sheng Liu, X. wang Li, L. K. Lin, Y. X. Shang, S. N. Shu, Y. Bai, M. Lu, G. Lu, J. K. Deng, W. J. Luo, L. J. Xiong, M. Liu, Y. X. Cui, L. P. Ye, J. F. Li, J. B. Shao, L. W. Gao, Y. Y. Wang, X. F. Wang, *World J. Pediatr.* **2020**, *16*, 232–239.
- [2] Y. Abo-zeid, R. A. Urbanowicz, B. J. Thomson, W. L. Irving, A. W. Tarr, M. C. Garnett, *Enhanced Nanoparticle Uptake into Virus Infected Cells: Could Nanoparticles Be Useful in Antiviral Therapy?*, **2018**.
- [3] Y. Abo-zeid, N. S. Ismail, G. R. McLean, N. M. Hamdy, *Eur. J. Pharm. Sci.* **2020**, *153*, 105465.
- [4] D. Bobo, K. J. Robinson, J. Islam, K. J. Thurecht, S. R. Corrie, *Pharm. Res.* **2016**, *33*, 2373–2387.
- [5] V. Sainz, J. Connot, A. I. Matos, C. Peres, E. Zupančič, L. Moura, L. C. Silva, H. F. Florindo, R. S. Gaspar, *Biochem. Biophys. Res. Commun.* **2015**, *468*, 504–510.
- [6] K. R. Wierzbinski, T. Szymanski, N. Rozwadowska, J. D. Rybka, A. Zimna, T. Zalewski, K. Nowicka-Bauer, A. Malcher, M. Nowaczyk, M. Krupinski, M. Fiedorowicz, P. Bogorodzki, P. Grieb, M. Giersig, M. K. Kurpisz, *Sci. Rep.* **2018**, *8*, 3682.
- [7] J. Zou, X. Wang, L. Zhang, J. Wang, *Chem. Res. Toxicol.* **2015**, *28*, 373–383.
- [8] P. S. Haddad, T. N. Britos, L. M. Li, L. D. S. Li, *J. Phys. Conf. Ser.* **2015**, *617*, 012002.
- [9] R. M. Patil, P. B. Shete, N. D. Thorat, S. V. Otari, K. C. Barick, A. Prasad, R. S. Ningthoujam, B. M. Tiwale, S. H. Pawar, *RSC Adv.* **2014**, *4*, 4515–4522.
- [10] G. F. L. Pereira, F. N. Costa, J. A. Souza, P. S. Haddad, F. F. Ferreira, *J. Magn. Magn. Mater.* **2018**, *456*, 108–117.
- [11] Wahajuddin, S. Arora, *Int. J. Nanomed.* **2012**, *7*, 3445–3471.
- [12] A. B. Seabra, T. Pasquoto, A. C. F. Ferrarini, M. D. C. Santos, P. S. Haddad, R. De Lima, *Chem. Res. Toxicol.* **2014**, *27*, 1207–1218.
- [13] S. Theerdhala, D. Bahadur, S. Vitta, N. Perkas, Z. Zhong, A. Gedanken, *Ultrason. Sonochem.* **2010**, *17*, 730–737.
- [14] G. Pizzino, N. Irrera, M. Cucinotta, G. Pallio, F. Mannino, V. Arcoraci, F. Squadrito, D. Altavilla, A. Bitto, *Oxid. Met.* **2017**, *2017*, 8416763.
- [15] A. Masoudi, H. R. Madaah Hosseini, M. A. Shokrgozar, R. Ahmadi, M. A. Oghabian, *Int. J. Pharm.* **2012**, *433*, 129–141.
- [16] A. B. Seabra, N. Durán, *J. Mater. Chem.* **2010**, *20*, 1624–1637.
- [17] A. B. Seabra, N. Durán, *Metals* **2015**, *5*, 934–975.
- [18] M. M. Molina, A. B. Seabra, M. G. De Oliveira, R. Itri, P. S. Haddad, *Mater. Sci. Eng. C* **2013**, *33*, 746–751.
- [19] S. Tarvirdipour, E. Vashghani-Farahani, M. Soleimani, H. Bardania, *Int. J. Pharm.* **2016**, *501*, 331–341.
- [20] T. Gelbrich, M. Feyen, A. M. Schmidt, *Macromolecules* **2006**, *39*, 3469–3472.
- [21] M. Auffan, L. Decome, J. Rose, T. Orsiere, M. De Meo, V. Briois, C. Chaneac, L. Olivi, J. L. Berge-Lefranc, A. Botta, M. R. Wiesner, J. Y. Bottero, *Environ. Sci. Technol.* **2006**, *40*, 4367–4373.
- [22] J. K. Patra, G. Das, L. F. Fraceto, E. V. R. Campos, M. D. P. Rodríguez-Torres, L. S. Acosta-Torres, L. A. Diaz-Torres, R. Grillo, M. K. Swamy, S. Sharma, S. Habtemariam, H. S. Shin, *J. Nanobiotechnol.* **2018**, *16*, 71.
- [23] Y. M. Huh, Y. W. Jun, H. T. Song, S. Kim, J. S. Choi, J. H. Lee, S. Yoon, K. S. Kim, J. S. Shin, J. S. Suh, J. Cheon, *J. Am. Chem. Soc.* **2005**, *127*, 12387–12391.
- [24] M. E. Sears, *Sci. World J.* **2013**, *2013*, 219840.
- [25] J. Shi, Z. Xiao, N. Kamaly, O. C. Farokhzad, *Acc. Chem. Res.* **2011**, *44*, 1123–1134.
- [26] G. Ge, H. Wu, F. Xiong, Y. Zhang, Z. Guo, Z. Bian, J. Xu, C. Gu, N. Gu, X. Chen, D. Yang, *Nanoscale Res. Lett.* **2013**, *8*, 215.
- [27] Y. Liu, Z. Chen, N. Gu, J. Wang, *Toxicol. Lett.* **2011**, *205*, 130–139.
- [28] P. Silvia Haddad, A. Barozzi Seabra, in *Iron Oxides Struct. Prop. Appl.*, **2012**, pp. 165–177.
- [29] L. H. Reddy, J. L. Arias, J. Nicolas, P. Couvreur, *Chem. Rev.* **2012**, *112*, 5818–5878.
- [30] H. Cohen, A. Gedanken, Z. Zhong, *J. Phys. Chem. C* **2008**, *112*, 15429–15438.
- [31] S. H. Hussein-Al-Ali, M. E. El Zowalaty, M. Z. Hussein, B. M. Geilich, T. J. Webster, *Int. J. Nanomed.* **2014**, *9*, 3801–3814.
- [32] S. Yoffe, T. Leshuk, P. Everett, F. Gu, *Curr. Pharm. Des.* **2012**, *19*, 493–509.
- [33] Z. R. Stephen, F. M. Kievit, M. Zhang, *NIH Public Access* **2011**, *14*, 330–338.
- [34] M. C. Santos, A. B. Seabra, M. T. Pelegrino, P. S. Haddad, *Appl. Surf. Sci.* **2016**, *367*, 26–35.
- [35] S. I. C. J. Palma, M. Marciello, A. Carvalho, S. Veintemillas-Verdaguer, M. del P. Morales, A. C. A. Roque, *J. Colloid Interface Sci.* **2015**, *437*, 147–155.
- [36] V. D. Chavan, V. P. Kothavale, S. C. Sahoo, P. Kollu, T. D. Dongale, P. S. Patil, P. B. Patil, *Phys. Condens. Matter* **2019**, *571*, 273–279.
- [37] S. Laurent, D. Forge, M. Port, A. Roch, C. Robic, L. Vander Elst, R. N. Muller, *Chem. Rev.* **2008**, *108*, 2064–2110.
- [38] M. Bloemen, W. Brullot, T. T. Luong, N. Geukens, A. Gils, T. Verbiest, *J. Nanopart. Res.* **2012**, *14*, 1100.
- [39] S. K. Jat, R. R. Bhattacharjee, *Microfluid. Nanofluidics* **2016**, *20*, 7.
- [40] K. Shameli, M. Bin Ahmad, S. D. Jazayeri, S. Sedaghat, P. Shabanzadeh, H. Jahangirian, M. Mahdavi, Y. Abdollahi, *Int. J. Mol. Sci.* **2012**, *13*, 6639–6650.
- [41] J. Zhang, S. Rana, R. S. Srivastava, R. D. K. Misra, *Acta Biomater.* **2008**, *4*, 40–48.
- [42] F. Monte, M. P. Morales, D. Levy, A. Fernandez, M. Ocan, *Langmuir* **1997**, *13*, 3627–3634.
- [43] R. Itri, J. Depeyrot, F. A. Tourinho, M. H. Sousa, *Eur. Phys. J. E* **2001**, *4*, 201–208.
- [44] H. P. Klug, L. E. Alexander, *X-ray Diffraction Procedures for Polycrystalline and Amorphous Materials*, John Wiley & Sons, Inc., New York, USA, **1954**.
- [45] C. Liu, J. Guo, W. Yang, J. Hu, C. Wang, S. Fu, *J. Mater. Chem.* **2009**, *19*, 4764.
- [46] A. Floris, C. Sinico, A. M. Fadda, F. Lai, F. Marongiu, A. Scano, M. Pilloni, F. Angius, C. Vázquez-Vázquez, G. Ennas, *J. Colloid Interface Sci.* **2014**, *425*, 118–127.
- [47] S. K. Balavandy, K. Shameli, D. R. B. A. Biak, Z. Z. Abidin, *Chem. Cent. J.* **2014**, *8*, 11.
- [48] R. Kumar, M. Nayak, G. C. Sahoo, K. Pandey, M. C. Sarkar, Y. Ansari, V. N. R. Das, R. K. Topno, Bhawna, M. Madhukar, P. Das, *J. Infect. Chemother.* **2019**, *25*, 325–329.
- [49] L. Gutierrez, X. Li, J. Wang, G. Nangmenyi, J. Economy, T. B. Kuhlenschmidt, M. S. Kuhlenschmidt, T. H. Nguyen, *Water Res.* **2009**, *43*, 5198–5208.
- [50] K. Murugan, J. Wei, M. S. Alsalhi, M. Nicoletti, M. Paulpandi, C. M. Samidoss, D. Dinesh, B. Chandramohan, C. Paneerselvam, J. Subramaniam, C. Vadivalagan, H. Wei, P. Amuthavalli, A. Jaganathan, S. Devanesan, A. Higuchi, S. Kumar, A. T. Aziz, D. Nataraj, B. Vaseeharan, A. Canale, G. Benelli, *Parasitol. Res.* **2017**, *116*, 495–502.

Submitted: May 28, 2021

Accepted: August 4, 2021